ELSEVIER

Journal of Power Sources 53 (1995) 175–183

JOURNAL OF POWER SOURCES

Paste structure and its influence on the agglomerate-of-spheres parameters of the PbO_2 electrode

E. Bashtavelova, A. Winsel

Universität Gesamthochschule Kassel, Heinrich-Plett-Straße, 34132 Kassel, Germany

Received 16 August 1994; accepted 2 September 1994

Abstract

During the past decade, the agglomerate-of-spheres (AOS) model has been developed to describe the behaviour of the PbO_2 electrode during cycling. Recently, the creation of the AOS has been described as an electrometasomatic process. In this process, a single 'sphere' at the end of an electronic path is a result of the action of the surface tension and its tendency to construct a sphere. This process can continue as long as the surface tension is sufficient to act against the internal friction. The so-called 'electroformative force' leads to an extension of the volume of the positive paste during the formation process. From a technological point of view, it is of interest to investigate the influence of the paste structure on the AOS parameters of the PbO_2 electrode. For this purpose, measurements are performed on PbO_2 produced from $3PbO \cdot PbSO_4 \cdot H_2O$ (3BS) and $4PbO \cdot PbSO_4$ (4BS) pastes. During formation of PbO_2, the electroformative forces cause an expansion of the electrode volume of the 3BS and 4BS pastes. Due to the 'pommes frites'-like structure of the 4BS mass, the formation process is different with respect to the velocity of building of the electronic conducting bridges within the electrode body. The formation process converts $PbSO_4$ on the outer surface of the 'pommes frites' to PbO_2, and leaves the internal region unaffected at first. The formation process bridges the cross points of the 'pommes frites'. Thus, an electronic and mechanic network is constructed. This leads to an electroformative force that is 3–4 times larger for 4BS than for 3BS paste. The apparent specific resistance of PbO_2 is twice as large for 4BS than for 3BS precursor paste. At the beginning of cycling, the 'unusual' increase of the force during discharge of the 4BS material shows that the reaction product, $PbSO_4$, is deposited within the PbO_2 electrode under formation of a mechanical stress in the AOS network. The cause for this is a difference in pore-size distribution between the '4BS' and '3BS' PbO_2. On average, the diffusion path for the lead ions is longer in the '4BS' material. The simultaneous measurement of polarization resistance and electronic-path resistance reveals the current distribution within the electrode during charge and discharge. It is concluded that during discharge and charge, the current distribution is almost homogeneous throughout the electrode, except at the end of discharge and the beginning of recharge when the current is constricted to the region near to the grid. The capacity of the constriction range is about 10% of the total capacity.

Keywords: Lead dioxide electrode; Paste structure; Agglomerate-of-spheres

1. Introduction

During the past decade, the agglomerate-of-spheres (AOS) model has been developed [1] in order to describe the behaviour of the PbO_2 electrode during cycling. This behaviour often leads to a disastrous and unexpected diminution of the capacity (so-called 'premature capacity loss'). The loss of capacity has proved to be relaxable, a property that can be explained by the AOS model. Recently, the creation of the AOS body has been described as an electrometasomatic process. In this process, the single sphere at the end of an electronic path results from the action of the surface tension and its tendency to construct a sphere. This process can continue for as long as the surface tension is sufficient to act against the internal friction. From this picture, the existence of a so-called electroformative force has been deduced. This results in an extension of the volume of the positive paste during the formation process. Using special equipment, it has been possible to measure the mechanical and electrical properties of the AOS electrode.

From a technological point of view, it is of interest to investigate the influence of the paste structure on the AOS parameters of the PbO_2 electrode. For this purpose, measurements have been performed on PbO_2

SSDI 0378-7753(94)01985-5

electrodes produced from tribasic lead sulfate ($3PbO \cdot PbSO_4 \cdot H_2O = 3BS$) and tetrabasic lead sulfate ($4PbO \cdot PbSO_4 = 4BS$) pastes. The results are reported in this paper.

2. Experimental set-up

The experimental set-up has been described in a previous paper [2]. It consists of a special electrochemical cell with integrated tension-testing equipment. The grid is bowl-like (Fig. 1) in order to contain the active material and a rod that is pressed slightly on the tablet of unformed paste. The force that is affected by the active material on the rod is measured during formation and cycling. Also, the direct current resistance between the rod and the bowl is measured continuously. The electrode potential is controlled with the aid of a new type of hydrogen electrode. The computerized experiments are performed inside a heat isolated compartment, which guarantees a uniform temperature during day and night. In all the experiments reported here, the current during formation and cycling was fed to the PbO_2 electrode via the bowl.

3. Formation process

During formation of PbO_2, the creation of the AOS structure takes place. A coherent electronic network is formed which is an electrometasomatic process that preserves the structure of the paste from which it has originated. During formation, a direct current is applied between the rod and the bowl and the resulting voltage drop is measured. From this, the resistance can be calculated. At the beginning of the formation process, the resistance consists of the solid-state resistance of the PbO_2 network and of an electrochemical part. This is true as long as the PbO_2 does not bridge the space between the bowl and the rod completely. The completion of the network is marked by a sharp decrease in the value of the resistance. The formation of the AOS structure causes the electroformative forces that promote an expansion of the volume of the paste. This effect seems to be strange since, during formation, the volume of the active material 'shrinks' theoretically. But those involved in the production process of lead/acid batteries know very well that overpasted PbO_2 electrodes tend to 'arch' during formation. This electroformative swelling proves that the structure of the AOS body needs additional space just like that of the lattice of ice when it freezes from water. This behaviour is equally true for 3BS- and 4BS-based pastes.

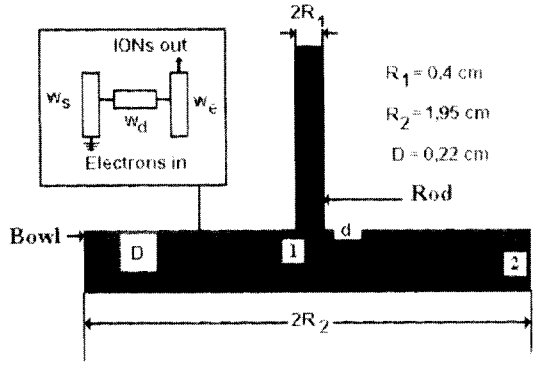

Fig. 1. Fronts of formation: type No. 1 = +pole on rod; type No. 2 = +pole on bowl.

3.1. Variation of the resistance

The formation processes of both 3BS and 4BS pastes are presented in Figs. 2 and 3, respectively. As expected, the curves of the resistance show a sharp decrease as soon as the electronic connection between the rod and the lead bowl through the growing PbO_2 bridges has been established. But the applied charge for this event shows that the formation process is different with respect to the velocity of the building of the electronic conducting bridges within the electrode body. Due to the 'pommes frites'-like structure of the 4BS mass, the formation process converts lead sulfate on the outer surface of the 'pommes frites' to PbO_2 and, at first,

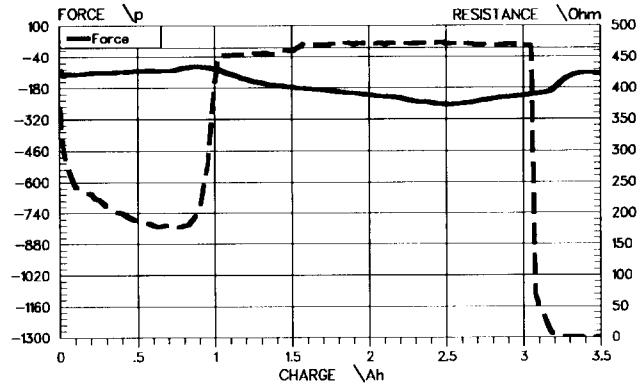

Fig. 2. Formation of 3BS paste. Current: 25 mA g^{-1}.

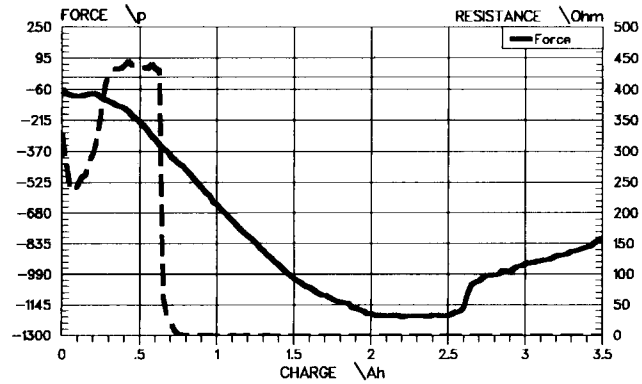

Fig. 3. Formation of 4BS paste. Current: 25 mA g^{-1}.

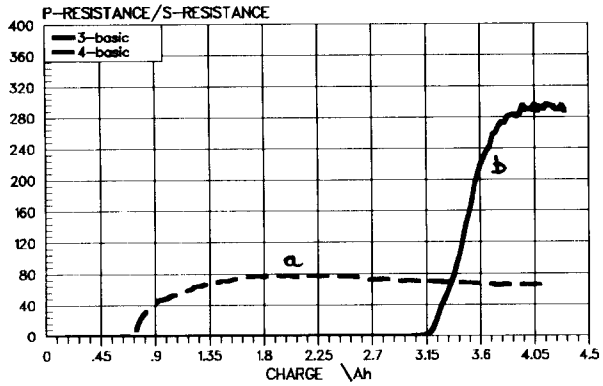

Fig. 4. Polarization resistance/solid-state resistance. Formation: 25 mA g^{-1}.

leaves the internal parts unaffected. The formation process quickly bridges the cross points of the 'pommes frites'. Thus, an electronic and mechanical network is constructed earlier than in case of the 3BS paste. This is confirmed by the data in Fig. 4. It shows the quotient 'polarization resistance/solid-state resistance' as a function of the applied charge. The polarization resistance is calculated from the actual polarization by dividing it by the applied current. For the 3BS curve, the quotient remains very small until nearly all of the material has been converted. Then its value increases quickly to about 300 and shows that the PbO_2 network is well established. In the case of the 4BS material, the bridging occurs as soon as a quarter of the charge has been applied. The quotient remains at about 80, however, and this indicates that the solid-state resistance of the electrode remains at a higher level.

3.2. Variation of the force

For 3BS and 4BS pastes, there is a marked difference in the development of the force during the formation process, as shown in Figs. 2 and 3. In the case of the 4BS material (Fig. 3), the force grows nearly proportional to the applied charge and is not affected by the completion of the solid-state bridges between the bowl and the rod which is indicated by a sharp decrease in the solid-state resistance. This shows that the formation process takes place all over the depth of the probe on the surface of the large 4BS crystals shown in Fig. 5(a). It also indicates that no internal dislocations occur in order to equilibrate pressure gradients in the electrode; the structure is very stable.

For 3BS paste (Fig. 2), the same gradation of the force is used as for 4BS material (Fig. 3). The force remains at a lower level and does not grow steadily as in the 4BS case. This means that the tendency of the electrode to enlarge its volume is much larger with 4BS material than with the 3BS counterpart. Electron micrographs of the formed 3BS material (Fig. 5(b)) show that pressure gradients within this structure may

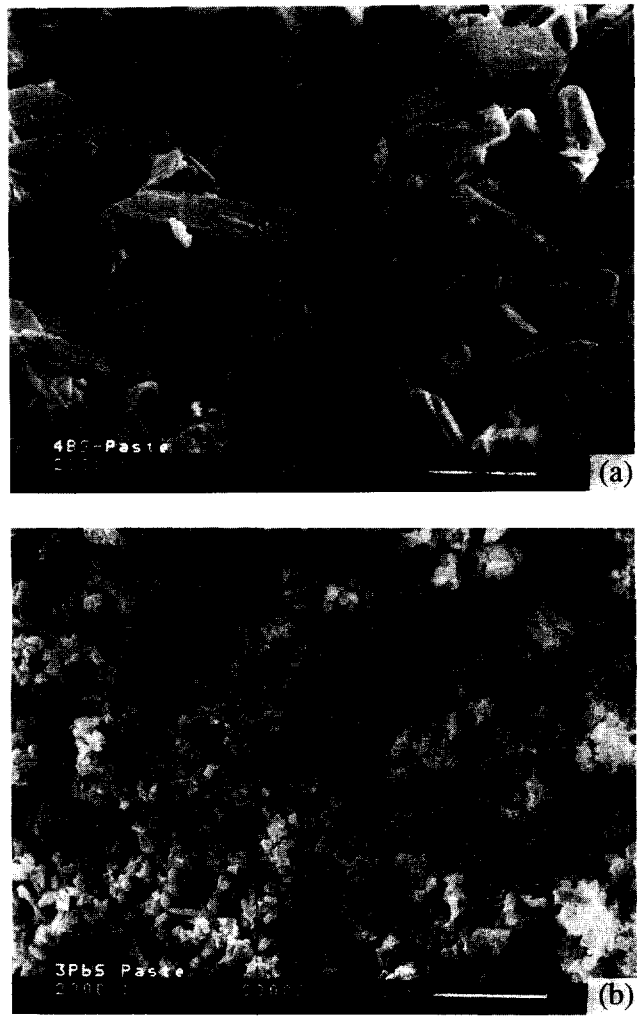

Fig. 5. Electronmicrographs of unformed paste: (a) 4BS; (b) 3BS.

effect dislocations of material as long as the PbO_2 network has not been completed throughout the entire electrode structure.

4. Cycling behaviour

4.1. First discharge after formation

In the first discharge immediately after formation, the capacity of the 4BS-based material is about 60% of that of the 3BS-based equivalent (see Figs. 6 and 7). The apparent specific resistance is very similar to that of the 3BS material, e.g., during discharge its value is almost less than during charge. During discharge, its value is nearly constant, but it increases sharply at the end of discharge. The resistance of the 4BS structure is nearly twice that of the 3BS material.

In Fig. 6, the force during discharge decreases rapidly, reaches a maximum at 65% of discharge, and increases again very quickly at the end of discharge. In Fig. 7, the force of the 3BS material exhibits the same be-

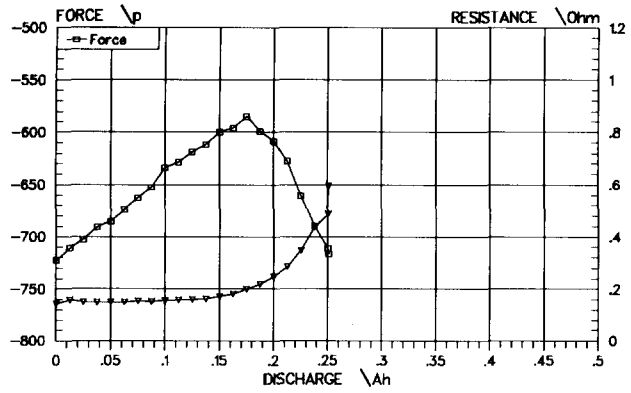

Fig. 6. First discharge after formation. 15 mA g^{-1}, via bowl. 4BS paste.

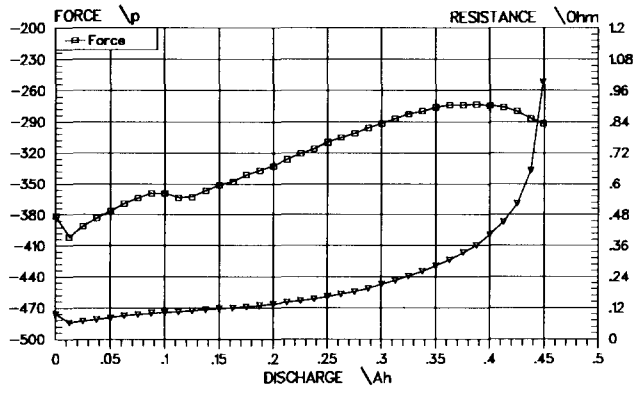

Fig. 7. First discharge after formation. 15 mA g^{-1}, via bowl. 3BS paste.

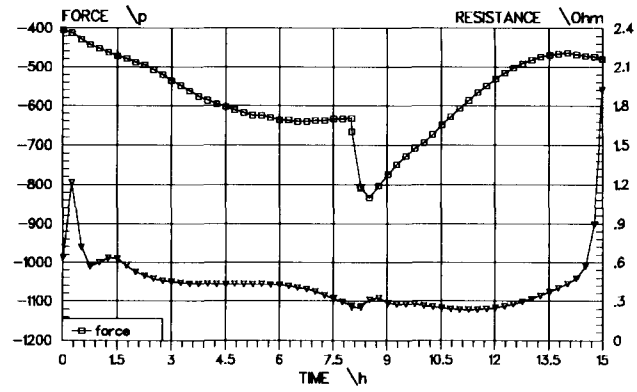

Fig. 8. First charge and second discharge. *I*-charge = 65 mA, *I*-discharge = 50 mA. 3BS paste.

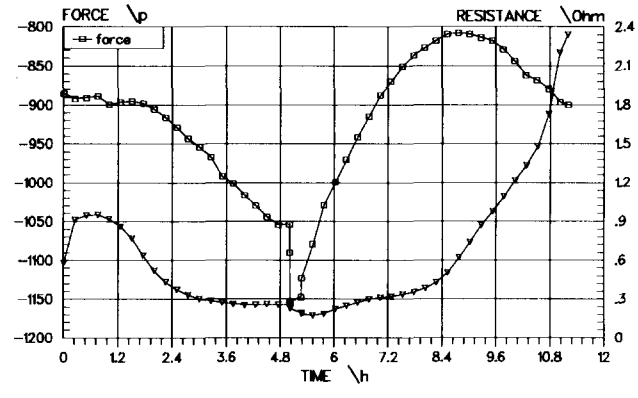

Fig. 9. First charge and second discharge. *I*-charge = 65 mA, *I*-discharge = 50 mA. 4BS paste.

haviour, although the maximum is less pronounced. Therefore our former explanation remains true, namely: during discharge the generated lead sulfate is deposited within the free-pore space without stretching of the PbO_2 network. At the end of discharge, however, the lead sulfate is deposited in places where its crystallization stretches the network and destroys the necks in the structure by a mechanical stress, or the necks are converted to lead sulfate by electrochemical corrosion directly.

4.2. First charge and second discharge

In Fig. 8, the force and resistance of the 3BS material are shown for the first charge–discharge cycle. As reported earlier, the solid-state resistance has its lowest values during discharge. Also, the force behaves as usual: its negative value, e.g., the pressure against the rod, decreases during most of the discharge time and shows by this effect that the reaction product lead sulfate is deposited stress-free inside the pore system. At the end of discharge, however, its curve shows a slight decrease after a maximum. The capacity of the electrode is about 0.35 Ah. In Fig. 9, both functions are demonstrated for the 4BS material. The capacity (0.3 Ah) is smaller than in the 3BS case, but larger than in the first discharge. The curve of the force still has a remarkable maximum. In the range between the maximum and the end of discharge, the resistance increases rapidly. This again indicates that the end of discharge may be effected by the mechanical interruption of the necks, or by their electrochemical corrosion and conversion to lead sulfate. For this 4BS material, the correlation between resistance, force and end-of-discharge is obvious.

4.3. First ten cycles

If the electrodes are cycled, the behaviour of the 4BS material becomes more and more equal to that of the 3BS variety. The variation of the force during discharge of a 3BS electrode is presented in Fig. 10. All curves behave similarly: the force decreases monotonously during the entire discharge process and ends in a minimum. Nevertheless, the force increases from cycle to cycle. The force in the 4BS electrode exhibits the same trend (Fig. 11), but its change per cycle is less. There seems to exist no tendency of the force to increase from cycle to cycle, contrary to that observed for 3BS material. From this, it can be concluded that

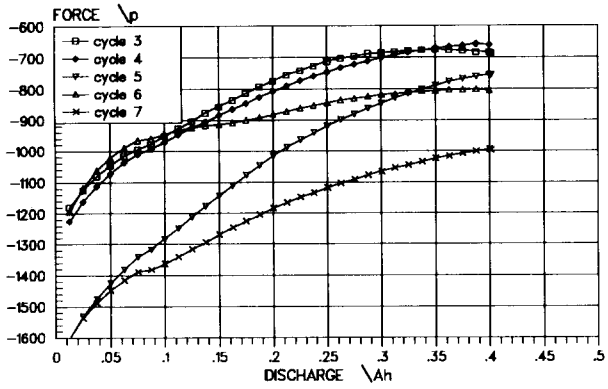

Fig. 10. Change of the force during discharge. I-discharge = 50 mA. 3BS paste.

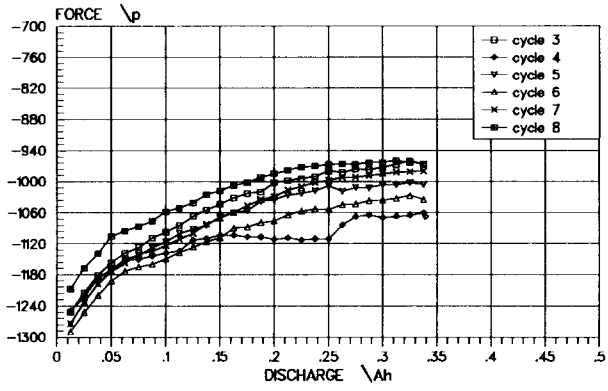

Fig. 11. Change of the force during discharge. I-discharge = 50 mA. 4BS paste.

the 4BS electrode has only a minor tendency to enlarge its volume during cycling. From a comparison of the development of the force from the formation to the eighth cycle, it can be seen that in the case of the 4BS material, the force after formation is high but changes only slightly thereafter, whereas in the case of the 3BS material, the force is low after formation but increases strongly from cycle to cycle. This difference is caused by a difference in the pore-size distributions. According to the passivation theory [3], different capacity behaviour of the two materials is expected with respect to the current density, but this has yet to be proved.

The development of the force of the 3BS material as a function of the charge during the first eight cycles is shown in Fig. 12. All curves have the same shape; namely, a decrease in the force at the beginning and an increase in the force till the end of the charge process. It can be seen that the force increases from cycle to cycle, and also exhibits a maximum. The 4BS material (Fig. 13) displays the same behaviour, but the changes of the force occur over a much narrower range.

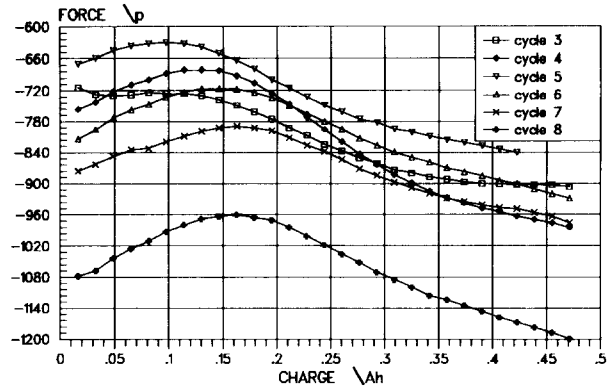

Fig. 12. Change of the force during charge. I-charge = 65 mA. 3BS paste.

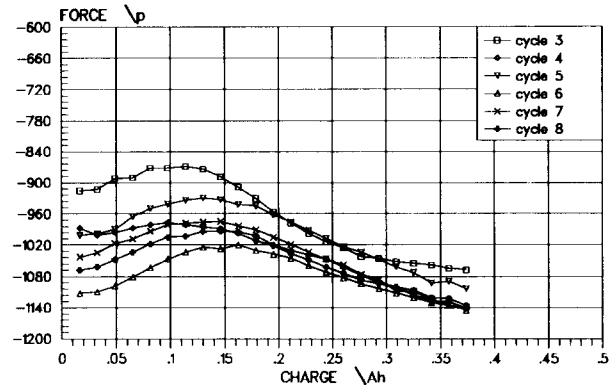

Fig. 13. Change of the force during charge I-charge = 65 mA. 4BS paste.

5. Current distribution in an agglomerate-of-spheres electrode

5.1. Formulation of the problem

The PbO_2 electrode proposed here consists of the solid-state agglomerate-of-spheres body with a liquid ion conductor, sulfuric acid, in its pores. Both phases are separated by the electrochemical double layer. For the cell shown in Fig. 1 with a cylindrical symmetry, a current of homogeneous density I flows in an axial direction of the coordinate z. If no current is applied to the cell, $I = 0$, the potential difference between the electrolyte phase $\phi_e(z)$ and the solid phase $\phi_s(z)$ is $\phi_e^0 - \phi_s^0$ at each point z. If the potential difference deviates from this value by a polarization η, a phase transition current of local density $j(z)$ is forced to flow. This is mainly proportional to the polarization $\eta(z)$ at this point, i.e.,

$$j(z) = -(1/w_d)\eta(z)$$

$$= -(1/w_d)[\phi_e(z) - \phi_s(z) - (\phi_e^0 - \phi_s^0)] \quad (1)$$

$$= -(1/w_d)[\varphi_e(z) - \varphi_s(z)];\ \varphi = \phi - \phi^0 \quad (2)$$

The term w_d is called the 'phase transition resistance'. Its value is specific to the unit volume of the positive electrode, i.e., $[w_d]=\Omega\ cm^3$. Its reciprocal $1/w_d$ is proportional to the specific internal surface of the PbO_2 electrode.

At a position z, the total current density I flows into the positive material via the grid at $z=0$ and spreads into a partial current $i(z)$ within the solid and a partial current $I-i(z)$ within the electrolyte phase. The current density $i(z)$ causes a potential drop at z that is proportional to w_s, the apparent specific resistance of the porous solid PbO_2, namely:

$$d\varphi_s(z)/dz = -w_s i(z) \tag{3}$$

At the same time, $I-i(z)$ causes a voltage drop within the electrolyte phase of the electrode that is proportional to the diaphragm resistance w_e:

$$d\varphi_e(z)/dz = -w_e[I-i(z)] \tag{4}$$

By differentiation of Eq. (3) and Eq. (4) it follows:

$$di(z)/dz = -(1/w_s)\ d^2\varphi_s/dz^2 \tag{5}$$

and

$$d[I-i(z)]/dz = -(1/w_e)\ d^2\varphi_e/dz^2 \tag{6}$$

By addition of both of these equations, we get with $I=$ const.:

$$-(1/w_s)\ d^2\varphi_s/dz^2-(1/w_e)\ d^2\varphi_e/dz^2=0 \tag{7}$$

With $w_e=$ const. and $w_s=$ const., it follows:

$$d^2(\varphi_e/w_e)/dz^2+d^2(\varphi_s/w_s)/dz^2=0 \tag{8}$$

and as a solution:

$$(\varphi_e/w_e)+(\varphi_s/w_s)=az+b \tag{9}$$

The boundary conditions are:

$$d(\varphi_e/w_e)/dz=0,\quad d(\varphi_s/w_s)/dz=-I,\quad \text{for } z=0$$

$$d(\varphi_e/w_e)/dz=-I,\quad d(\varphi_s/w_s)/dz=0,\quad \text{for } z=D$$

D is the position of the geometric surface of the positive electrode opposite to the negative one, e.g., D is the thickness of the positive electrode.

From this, it follows that $a=-I$ and

$$(\varphi_e/w_e)+(\varphi_s/w_s)=-Iz+b \tag{10}$$

Now, if Eq. (5) is subtracted from Eq. (6), then:

$$2di(z)/d_z = d^2(\varphi_e/w_e)/dz^2-d^2(\varphi_s/w_s)/dz^2 \tag{11}$$

The continuation equation is $di(z)/dz=-j(z)$, and with Eq. (2) yields:

$$d^2(\varphi_e/w_e)/dz^2-d^2(\varphi_s/w_s)/dz^2 = 2[(w_e/w_d)(\varphi_e/w_e)-(w_s/w_d)(\varphi_s/w_s)] \tag{12}$$

In order to solve this equation, we make use of Eq. (8) and Eq. (10) and find:

$$d^2(\varphi_e/w_e)/dz^2-[(w_s+w_e)/w_d)](\varphi_e/w_e) -(w_s/w_d)(Iz-b)=0 \tag{13}$$

The solution to the problem is formulated by the following equation:

$$\varphi_e/w_e = A_1\exp\{\lambda z\}+A_2\exp\{-\lambda z\}+K_e z+K^0 \tag{14}$$

By insertion of Eq. (14) in Eq. (13) it follows:

$$A_1\lambda^2\exp\{\lambda z\}+A_2\lambda^2\exp\{-\lambda z\} -[(w_s+w_e)/w_d)][A_1\exp\{\lambda z\} +A_2\exp\{-\lambda z\}+K_e z+K^0] -(w_s/w_d)(Iz-b)=0 \tag{15}$$

By comparison of the coefficients, we get:

$$\lambda^2-[(w_s+w_e)/w_d)]=0 \tag{16}$$

5.2. Penetration depth Λ

$\Lambda=\lambda^{-1}$ is called 'the penetration depth' of the current into the porous structure of the electrode. Its meaning becomes obvious by a simple transformation of Eq. (16):

$$w_d/\Lambda=(w_s+w_e)\Lambda \tag{17}$$

$$\Lambda=\sqrt{w_d/(w_s+w_e)} \tag{18}$$

The penetration depth Λ describes that zone of an electrode in which the phase transition resistance per unit geometric surface, w_d/Λ, is equal to the sum of electronic and ionic resistance, $(w_s+w_e)\Lambda$, of the entire structure. If Eq. (17) is divided by the cross section $Q=\pi R_2^2$ of the electrode, the left term $w_d/(Q\Lambda)$ can be identified with the 'effective charge-transfer resistance' $W_{d,\Lambda}$ of the electrode. Except for the factor (Λ/D), the term on the right hand side of Eq. (17), $[(w_s+w_e)D/Q](\Lambda/D)$, is equal to the sum of the solid-state resistance $W_s=w_sD/Q$, and of the measurable diaphragm resistance $W_e=w_eD/Q$ of the electrode. Therefore, Eq. (19) can be written instead of Eq. (17):

$$W_{d,\Lambda}/(W_s+W_e)=\Lambda/D \tag{19}$$

This equation very simply shows that the penetration depth, Λ, is information that is also included in the experiments reported here. During the direct-current charge and discharge reaction by a current J, the potential $\varphi(J, t)$ is measured as a function of the time with the aid of a reference electrode. Its deviation from the equilibrium value, φ^0, is called the overvoltage. The overvoltage as the driving force is divided by the current J and the result is called the 'polarization resistance' of the electrode $W'_{d,\Lambda}$. The prime indicates that this polarization resistance includes some parts of the diaphragm and of the solid-state resistance that are involved

in the current distribution. But these are only parts of the W_s value, which is steadily measured in our experiment. The same is true for the diaphragm resistance, which we are able to calculate during the experiment. Therefore, we can conclude:

$$W_{d,\Lambda} < W'_{d,\Lambda} < W_{d,\Lambda} + W_s + W_e \quad (20)$$

$$W_{d,\Lambda}/(W_s+W_e) < W'_{d,\Lambda}/(W_s+W_e) < W_{d,\Lambda}/(W_s+W_e)+1 \quad (21)$$

and according to Eq. (19):

$$\Lambda/D < W'_{d,\Lambda}/(W_s+W_e) < \Lambda/D+1 \quad (22)$$

This equation allows Λ/D to be determined from our measurements, although W_e is not measured directly. The conductivity of sulfuric acid is about $\kappa = 0.83\ \Omega^{-1}\ cm^{-1}$, the electrolyte-filled pore volume is $P=0.53$, the tortuosity factor $t=1/P=2$. With these values, $w_e = t/[P\kappa] = 2/[0.53\times 0.83] = 4.55\ \Omega$ cm. The thickness of the probe is $D=0.22$ cm; the cross section is $Q=3.14$ cm^2. Therefore, $W_e = w_e\ D/Q = 4.55\times 0.22/3.14\ \Omega = 0.32\ \Omega$.

W_s is even smaller than W_e, but both are changing during charge and discharge. Due to the AOS model and from these measurements, it is known that W_s remains at a low level during nearly all the discharge process. W_e will be affected by the formation of lead sulfate during discharge, but the same is true for $W'_{d,\Lambda}$, since the solid lead sulfate, which is deposited within the pores, acts as a diaphragm and hinders the charge transfer [4,6].

5.3. More about current distribution

By comparison of the coefficients in Eq. (14), the following expressions can be derived:

$$-(w_s+w_e)/w_d)K_e - w_s/w_d I = 0 \quad (23)$$

thus: $K_e = -Iw_s/(w_s+w_e)$

$$-K^0(w_s+w_e)/w_d + b(w_s/w_d) = 0 \quad (24)$$

thus: $K^0 = bw_s/(w_s+w_e)$

By adaptation of the boundary conditions, the following equations can be obtained for the potentials at $z=0$ in the solid phase (grid) and for $z=D$ in the liquid phase (position of the reference electrode) and its difference:

$$\varphi_e(D) - \varphi_s(0) = -I[w_s \exp\{-D/\Lambda\} + w_e] \times [w_s + w_e \cosh\{D/\Lambda\}]/[\sinh\{D/\Lambda\}(w_s+w_e)/\Lambda] - (w_s w_e ID/\Lambda + Iw_s[w_e \exp\{-D/\Lambda\} + w_s])/[(w_s+w_e)/\Lambda] \quad (25)$$

5.4. Definition of the polarization resistance of the electrode

It is useful to define the specific polarization resistance R_P of the electrode as used in these experiments. For this reason, the potential difference in Eq. (25) is divided by the current density I. This gives:

$$R_P = [\varphi_e(D) - \varphi_s(0)]/I \quad (26)$$

$$R_P(w_s+w_e)/\Lambda = -[w_s \exp\{-D/\Lambda\} + w_e] \times [w_s + w_e \cosh\{D/\Lambda\}]/[\sinh\{D/\Lambda\}] - w_s w_e D/\Lambda - w_s[w_e \exp\{-D/\Lambda\} + w_s] \quad (27)$$

From this last equation, it can be seen that the influence of the electronic resistance w_e of the agglomerate-of-spheres is weighted exponentially by the penetration depth compared with the influence of the diaphragm resistance w_e. $\Lambda^2 = w_d/(w_s+w_e)$ is symmetric in w_s and w_e and both determine the penetration depth Λ, together with the charge transfer resistance w_d. The position of this zone is determined, however, by the largest one of these values: if, for example, the electronic resistance w_e is dominant rather than the ionic one, the current lines will be restricted to a zone near $z=0$, e.g., near to the grid; if the diaphragm resistance is dominant, the constriction of the current lines takes place near to the geometric surface at $z=D$.

5.5. Special cases of current distribution

Two special cases are discussed here. The first concerns deep penetration $D/\Lambda \ll 1$, $\exp\{-D/\Lambda\} = 1 - D/\Lambda$, and $\exp\{D/\Lambda\} = 1 + D/\Lambda$. Furthermore, $\cosh\{D/\Lambda\} \approx 1$; $\sinh\{D/\Lambda\} \approx D/\Lambda$. Then:

$$R_P = -(w_s+w_e)\Lambda^2/D - w_s w_e D/(w_s+w_e) - w_s\Lambda \quad (28)$$

By inserting $\Lambda^2 = w_d/(w_s+w_e)$

$$R_P = -w_d/D - w_s w_e D/(w_s+w_e) - \sqrt{[w_d w_s^2/(w_s+w_e)]} \quad (29)$$

Eq. (29) shows that the polarization resistance consists of three parts that are connected in series. The first represents the charge-transfer resistance of the electrode under completely uniform current distribution. The second is the parallel combination of the diaphragm resistance and of the electronic resistance of the AOS. The third does not depend on the electrode thickness D. Its value increases proportional to $\sqrt{w_d}$, but its influence increases with increasing electronic resistance. This case appears to represent experiments of the type reported here.

The second special case is represented by a small value of the penetration depth Λ compared with the thickness D of the electrode. Then:

$\{D/\Lambda\} \gg 1$, $\exp\{-D/\Lambda\} \approx 0$, $\cosh\{\}/\sinh\{\} = 1$ and

$$R_P = -w_e\Lambda/(w_s+w_e) - w_e w_s D/(w_s+w_e) \quad (30)$$

$$= -[w_e/(w_s+w_e)][w_d/(w_s+w_e)]^{1/2} - w_e w_s D/(w_s+w_e) \quad (31)$$

Now, the polarization resistance is determined by a series-connection of two representative resistivities. As in the case before, the second term is the parallel resistance of the diaphragm resistance and of the electronic resistance of the electrode of thickness D. The first term is an additional one and independent of the electrode thickness.

5.6. Current distribution in present experiments

Eq. (22) combines the measured polarization resistance with the sum of the diaphragm and the measured solid-state resistance of the electrode used here (Fig. 1). The diaphragm resistance has, according to calculations, a value of about 0.3 Ω and will change a little during charge, as well as during discharge, due to the change of both the electrolyte concentration and the pore volume by the deposition or solution of lead sulfate. This change will be small, however, compared with the change in the solid state resistance W_s which is expected to increase to unlimited values if even one layer of necks in the electronic path is corroded. The polarization resistance $W'_{d,\Lambda}$ will be affected strongly by the electrodeposition of a lead sulfate diaphragm which, due to the passivation model, impedes the diffusion of lead ions away from the surface in a reaction-limiting way 4,5].

Eq. (22) is the basis of forthcoming considerations of the current distribution in PbO_2 electrodes. To refresh the reader's memory:

$$\Lambda/D < W'_{d,\Lambda}/(W_s+W_e) < \Lambda/D+1 \quad (22)$$

In this equation, if W_e is omitted beneath W_s, the resulting quotient $W'_{d,\Lambda}/W_s$ will be representative for the current distribution as long as W_s is large in comparison with W_e. Therefore, it is not possible to detect constrictions of the current that are due to a poor conductivity of the electrolyte and that are concentrated on the surface in the position $z=D$. Nevertheless, if the constriction is such that a surface layer of lead sulfate of thickness Λ is produced near to the grid, this quotient will show values between Λ/D and $\Lambda/D+1$. For example, if $D=0.22$ cm and $\Lambda=0.01$ cm, $\Lambda/D=0.045$ and the value of the quotient is expected to be between 0.05 and 1.05.

5.6.1. Current distribution during charge

In Fig. 14, the quotient $W'_{d,\Lambda}/W_s$ is shown as a function of the charge for six consecutive cycles for

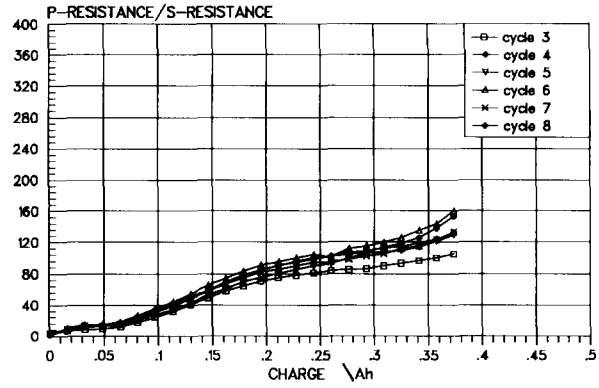

Fig. 14. Polarization resistance/solid-state resistance. I-charge = 65 mA. 4BS paste.

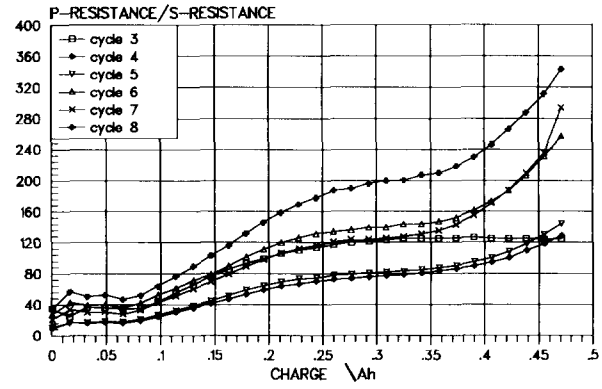

Fig. 15. Polarization resistance/solid-state resistance. I-charge = 65 mA. 3BS paste.

the 4BS material. All curves behave very similarly: at the beginning the quotient starts with low values (for example, 1.41) and rises quickly up to a plateau at about 15% of the total charge. This range is correlated to the reconstruction of necks that have been destroyed at the end of the preceding discharge process. After the plateau, the quotient increases linearly with the charge to a second plateau. A plateau can be observed if the polarization resistance and the solid-state resistance of the probe are both constant, or if both show the same proportionality to the charge. At the end of the charge reaction, when oxygen is evolved, the values of the quotient remain in the range 100–160.

The same relation is shown for the 3BS electrode in Fig. 15. The very first values show a certain scattering at higher values (>10) and all curves exhibit the same shape as the 4BS equivalents. At the end of charge, the quotient increases up to values in the range 120–350. This indicates an advantage of the 3BS material compared with the 4BS variety. Except for this observation,

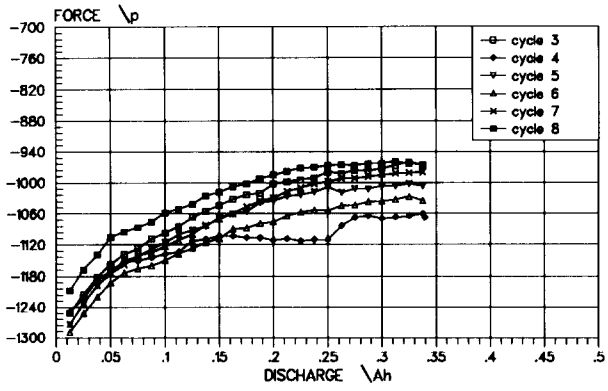

Fig. 16. Polarization force/solid-state resistance. *I*-discharge = 50 mA. 4BS paste.

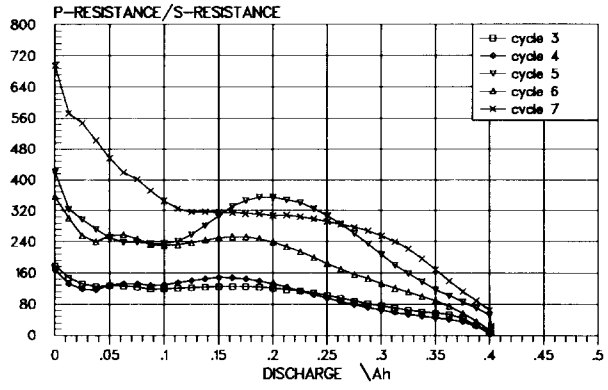

Fig. 17. Polarization resistance/solid-state resistance. *I*-discharge = 50 mA. 3BS paste.

it is concluded that no principal difference exists with respect to the current distribution between the 3BS and 4BS material.

5.6.2. *Current distribution during discharge*

The quotient $W'_{d,\Lambda}/W_s$ is presented in Fig. 16 as a function of the discharge for the same six consecutive cycles of 4BS material. All curves exhibit a similar shape, namely, a sharp decrease to a minimum at about 15% of discharge followed by a slight maximum at about 30% of discharge. Thereafter, the quotient decreases in proportion to the discharge and ends with values in the range 1.1–1.6. These values show that at the very end of discharge of the 4BS electrode, a constriction of the current lines takes place in a small part of the electrode near to the grid. Until this occurs, however, the current is distributed nearly constantly over the internal surface.

The quotient is shown for six consecutive discharge cycles of 3BS material in Fig. 17. At the beginning, the value decreases until 10–20% of the total charge is extracted. Again, a slight maximum can be observed, followed by a linear decrease to the end of discharge. The final values are in the range 5–25 and are much larger than in the 4BS case. This indicates that the discharge reaction of the 3BS material is not effected by peculiarities near to the grid or on top of the grid surface.

Acknowledgements

The authors are indebted to the 'Herbert-Quandt-Stiftung' of Varta Batterie AG, and to the European Advanced Lead–Acid Battery Consortium (Brite-Euram project BE 7297), a program of the Internation Lead Zinc Research Organization, Inc., for support. Assistance given by Mr A. Cooper (European Economic Interest Group) and Dr. E. Meissner (Varta Batterie AG) is gratefully acknowledged. Thanks are also due to Dr K. Salomon, Mr D. Bechtold, Mr D. Metzeltin, Mr. E. Rosskopf and Mr J. Vollbert of Varta Batterie AG for their help in preparing and analyzing of the electrodes.

References

[1] A. Winsel, E. Voss and U. Hullmeine, *J. Power Sources, 30* (1990) 209–226.
[2] E. Bashtavelova and A. Winsel, *J. Power Sources, 46* (1993) 219–230.
[3] A. Winsel, U. Hullmeine and A. Voss, *J. Power Sources, 2* (1977) 369–385.
[4] A. Winsel, *Ber. Bunsenges. Phys. Chem.*, (1975) 827–836.
[5] W. Kappus and A. Winsel, *J. Power Sources, 8* (1982) 159–173.
[6] T.G. Chang, *J. Electrochem. Soc., 131* (1984) 1755–1762.